ELSEVIER

Journal of Organometallic Chemistry 655 (2002) 227–232

Journal of Organometallic Chemistry

www.elsevier.com/locate/jorganchem

Phosphine substituted $Ru_3(\mu\text{-dppm})(CO)_{10}$: structural trends within $[Ru_3(\mu\text{-dppm})(PR_3)(CO)_9]$ (R = Et, Ph, Cy and Pr^i)

A. Asgar Torabi [1], Anthony S. Humphreys, George A. Koutsantonis *, Brian W. Skelton, Allan H. White

Department of Chemistry, University of Western Australia, 6009 Nedlands, WA, Australia

Received 23 January 2002; accepted 19 April 2002

Abstract

The complexes $[Ru_3(\mu\text{-dppm})(PR_3)(CO)_9]$ (R = Et, Ph, Cy, Pr^i} were prepared from $[Ru_3(\mu\text{-dppm})(CO)_{10}]$ by simple phosphine substitution reactions at room temperature and their structures determined by single crystal X-ray studies. Variations in the Ru–Ru bond adjacent to the phosphine ligand suggest the enhanced reactivity of $[Ru_3(\mu\text{-dppm})(CO)_{10}]$ over the parent carbonyl $[Ru_3(CO)_{12}]$ to be consequent on the inability of $[Ru_3(\mu\text{-dppm})(CO)_{10}]$ to effectively relieve steric congestion imposed by the presence of the bulky, bidentate dppm ligand.

Keywords: Ruthenium; Carbonyl substitution; Cluster; Phosphine

1. Introduction

The chemistry of $[Ru_3(\mu\text{-dppm})(CO)_{10}]$ (dppm = 1,2-bis (diphenylphosphino)methane) (**1**) [1], is characterised by the easy addition of numerous groups without prior activation of the cluster [2–5]. The complex readily undergoes facile ligand transformation, eliminating benzene and orthometallating another phenyl substituent [6–8].

Thus, this activated cluster provides an ideal starting material for the formation of higher nuclearity clusters. In using **1** as the framework upon which to build alkynylide clusters through the reaction with mononuclear metal alkynyls such as *trans*-$[Ni(C_2SiMe_3)_2(PEt_3)_2]$ it was observed that PEt_3 was transferred to **1**. The new trinuclear complex, $[Ru_3(\mu\text{-dppm})(CO)_9(PEt_3)]$ (**2a**), exhibiting some potentially interesting behaviour. In order to explore this more fully, other substituted clusters with phosphine ligands having differing steric requirements were prepared for comparison, $[Ru_3(\mu\text{-dppm})(CO)_9(PR_3)]$ (R = Cy, **2b**; Ph, **2c**; Pr^i, **2d**), supported by room temperature single crystal X-ray structure determinations.

2. Experimental

2.1. General procedures

The reactions were conducted under an atmosphere of high purity argon using standard Schlenk techniques and tetrahydrofuran (thf) dried over potassium metal. $[Ru_3(\mu\text{-dppm})(CO)_{10}]$ was prepared using the published procedure [9]. NMR spectra were measured on Varian Gemini 200 (operating at 200 and 50.3 MHz for ^1H and ^{13}C) and Bruker ARX 500 (operating at 202.46 MHz for ^{31}P) spectrometers.

2.2. Preparation of $[Ru_3(\mu\text{-dppm})(CO)_9(PR_3)]$ (2)

2.2.1. R = Et (2a)

To a solution of **1** (0.100 g, 0.103 mmol) in thf (20 ml) was added solid $[Ni(C_2SiMe_3)_2(PEt_3)_2]$ (0.051 g, 0.104

---

* Corresponding author. Fax: +619-380-7247

E-mail address: gak@chem.uwa.edu.au (G.A. Koutsantonis).

[1] On leave from Zanjan university, Republic of Iran.

0022-328X/02/$ - see front matter
PII: S0022-328X(02)01567-X

mmol) and the resulting solution stirred for 1 h. The solvent was removed in vacuo and the red–orange residue was crystallised from CH_2Cl_2–MeOH giving deep red crystals of **2a** (0.071 g, 65%), in two crops. Anal. Calc. for $C_{40}H_{37}O_9P_3Ru_3 \cdot CH_2Cl_2$: C, 43.08; H, 3.44. Found: C, 43.69; H, 3.44%. IR (C_6H_{12}): ν(CO) 2050m, 1990s, 1973s, 1939m cm^{-1}. ^{1}H-NMR (C_6D_6) δ 0.75 (m, 3H, PCH_2CH_3), 1.43 (m, 2H, PCH_2CH_3), 4.14 (t, $^2J_{PH} = 10$ Hz, 2H, PCH_2P), 6.9–7.4 (m, 20H, $PhPCH_2$). ^{31}P-NMR ($CDC1_3$) δ 15.9 (br s, dppm), 24.1 (t, $^3J_{PP} = 7.8$ Hz, PEt_3). FABMS (NOBA–CH_2C1_2) m/z 1059, [M$^+$]; 1031–807, [M–nCO]$^+$ $n = 1$–9.

Complex **2a** is better prepared by the general route described below which gives spectroscopically identical material.

2.3. General synthesis

To a solution of **1** in thf (20 ml) was added phosphine and the reaction stirred. After the reaction appeared complete (TLC) the solvent was removed in vacuo and the residue chromatographed (TLC, 1/5 acetone–hexanes) to remove unreacted starting material and the band corresponding to the product was crystallised from CH_2Cl_2–hexanes.

2.3.1. R = Cy (2b)

Using the above general method, **1** (0.107 g, 0.11 mmol), PCy_3 (0.052 g, .45 mmol) for 36 h gave **2b** (0.077 g, 66%). Anal. Calc. for $C_{52}H_{55}O_9P_3Ru_3$: C, 51.18; H, 4.54;. Found: C, 50.89; H, 4.48%. IR (C_6H_{12}): ν(CO) 2051m, 1994s, 1980sh, 1976s, 1942m cm^{-1}. ^{1}H-NMR (C_6D_6) δ 1.58–2.25 (m, 33H, PC_6H_{11}), 4.14 (t, $^2Jp_H =$ 10 Hz, 2H, PCH_2P), 6.9–7.5 (m, 20H, $PhPCH_2$). ^{31}P-NMR ($CDC1_3$) δ 14.9 (m, dppm), 48.5 (t, $^3J_{PP} = 7.5$ Hz, PCy_3). FABMS (NOBA–CH_2C1_2) m/z 1220, [M$^+$]; 1193–969, [M–nCO]$^+$ $n = 1$–9.

2.3.2. R = Ph (2c)

Using the above general method, **1** (0.109 g, 0.11 mmol), PPh_3 (0.052 g, 0.12 mmol) for 24 h gave **2c** (0.098 g, 73%). The m.p. and FABMS were identical with those reported in the literature [4].

2.3.3. R = PPr^i_3 (2d)

Using the above general method, **1** (0.500 g, 0.517 mmol), PPr^i_3 (0.083 g, 0.517 mmol) for 24 h gave **2d** (0.36 g, 63%). Anal. Calc. for $C_{43}H_{43}O_9P_3Ru_3$: C, 45.94; H, 3.94;. Found: C, 46.41; H, 3.91%. IR (CH_2C1_2): ν(CO) 2047W, 1990sH, 1973s, 1942w cm^{-1}. ^{1}H-NMR ($CDC1_3$) δ 1.26 (dd, $^3J_{PH} = 14$ Hz, $^3J_{HH} = 7$ Hz, 18H, $PCHCH_3$), 1.40(m, 3H, $PCHCH_3$), 4.22 (t, $^2J_{PH} = 10$ Hz, 2H, PCH_2P), 7.3–7.4 (m, 20H, $PhPCH_2$). ^{31}P-NMR ($CDC1_3$) δ 14.84 (m, dppm), 48.5 (qt, PPr^i_3,). FABMS (NOBA–CH_2Cl_2) m/z 1102, [M$^+$]; 1073–949, [M–nCO]$^+$ $n = 1$–9.

2.4. Structure determinations of 1 and 2

For **2a**–**c**, unique room temperature single counter diffractometer data sets were measured ($2\theta - \theta$ scan mode, $2\theta_{max}$ as specified; monochromatic Mo–K$_\alpha$ radiation, $\lambda = 0.71073$ Å; T = 295 K), yielding N independent reflections, N_0 of these with $I > 3\sigma(I)$ considered 'observed' and used in the full-matrix least-squares refinement after gaussian absorption correction. For **1**, **2d**, full spheres of CCD area detector diffractometer data were measured at ca. 153 K (Bruker AXS instrument, ω-scans) yielding N_{total} reflections, merging to N_{unique} (R_{int} quoted) after 'empirical'/multiscan absorption correction (proprietary software), the observed criterion being $F > 4\sigma(F)$. Anisotropic thermal parameter forms were refined for the non-hydrogen atoms, $(x, y, z, U_{iso})_H$ being constrained at estimated values. Conventional residuals R, R_w (statistical weights) on $|F|$ are quoted at convergence. Neutral atom complex scattering factors were employed, computation using the XTAL3.4 program system [10]. Pertinent results are given in the figures (Fig. 1) and tables (Tables 1 and 2), the former showing 20 (295 K) or 50% (153 K) displacement amplitude ellipsoids for the non-hydrogen atoms, the hydrogen atoms having arbitrary radii of 0.1 Å.

Individual variations, idiosyncrasies, abnormalities are as follows:

1) Complex **1**: this complex has been the subject of a previous room temperature study, cell and coordinate setting providing the basis for the present study.
2) Complex **2a** (triclinic): the crystal decomposed by ca. 10% during data collection and data are scaled accordingly. Data were weak and would only support meaningful anisotropic thermal parameter form refinement for Ru and P. The ethyl groups on molecule **2** were disordered and refined with constrained geometries and site occupancies set at 0.5. A similar disorder was observed in the orthorhombic phase, resolvable for the inner methylene components of each substituent only.
3) Complex **2c**: difference map residues were modelled as a pair of dichloromethane solvent molecules, each disordered over a pair of sites with equal occupancy; isotropic thermal parameter forms were refined. In view of the long axis, an extended counter arm was used in data collection.

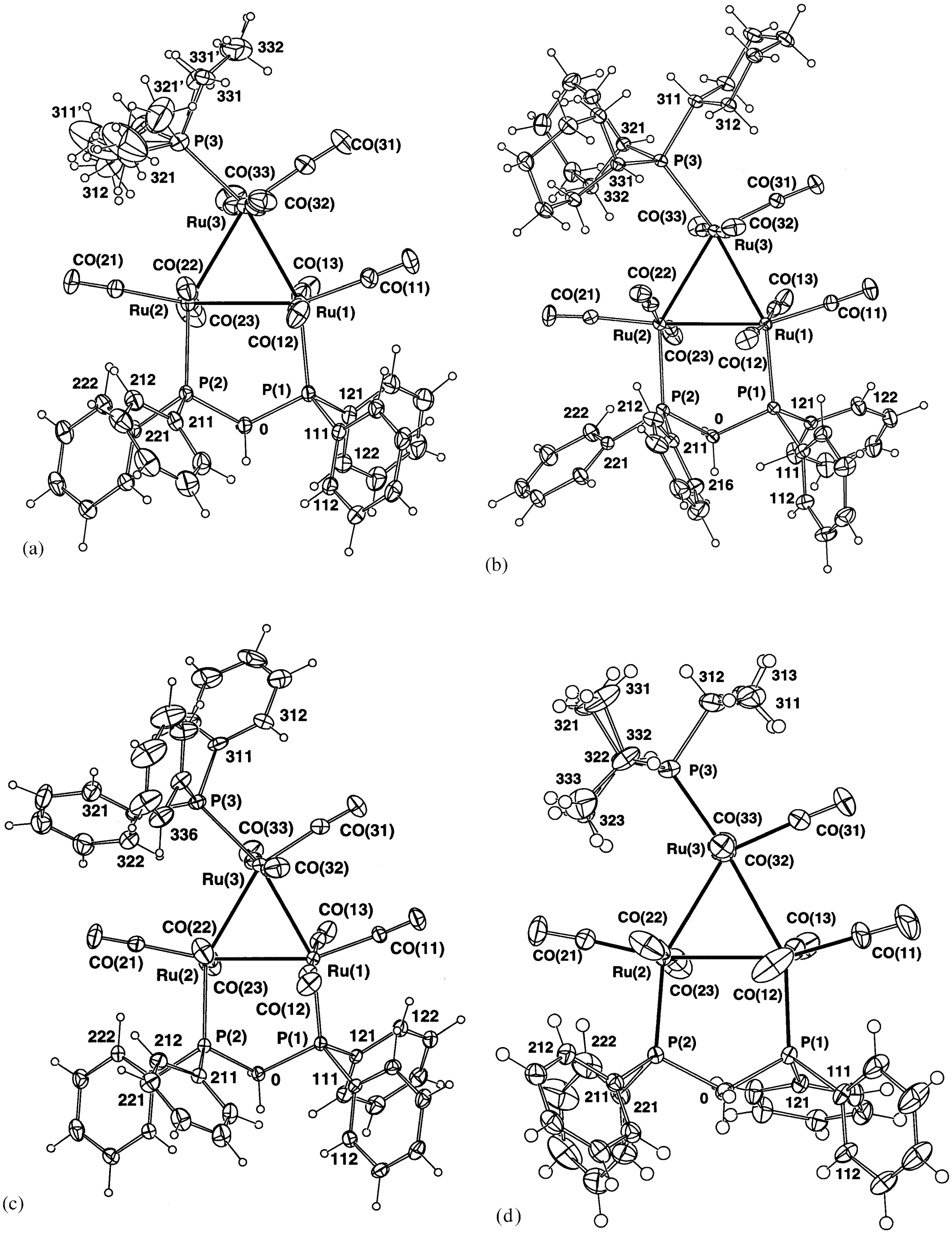

Fig. 1. (a)–(d) Molecular Structure of **2a** (orthorhombic form), **2b**, **2c**, **2d**.

3. Results and discussion

3.1. Syntheses

Complexes **2a**–**d**, all containing the familiar triangular Ru_3 core with all phosphorus atoms equatorial, were prepared by simple phosphine substitution reactions at room temperature. In addition **2a** was prepared from the unusual abstraction of PEt_3 from *trans*-[Ni(C_2SiMe_3)$_2$(PEt_3)$_2$] giving presumably *trans*-[Ni(C_2SiMe_3)$_2$(PEt_3)(CO)] and the ruthenium cluster. To the best of our knowledge there have been no previous reports of **2a** (either form), **d** or complete characterisation of **2b**. However, the synthesis of **2c** has been reported by various procedures which require elevated temperatures [11,12] or initiation by Me_3NO [4].

3.2. Crystal structures

Two phases were found for Complex **2a**. The triclinic $P\bar{1}$ phase crystallised with two complete molecules in the asymmetric unit, but its determination is inferior and is

Table 1
Crystal and refinement data for [$Ru_3(\mu\text{-dppm})(CO)_9(L)$]

Complex	**1**	**2a**	**2a**	**2b**	**2c**($\cdot$ 2CH_2Cl_2)	**2d**
L	CO	PEt_3	PEt_3	PCy_3	PPh_3	PPr^i_3
Formula	$C_{35}H_{22}O_{10}P_2Ru_3$	$C_{40}H_{37}O_9P_3Ru_3$	$C_{40}H_{37}O_9P_3Ru_3$	$C_{52}H_{55}O_9P_3Ru_3$	$C_{54}H_{41}Cl_4O_9P_3Ru_3$	$C_{43}H_{43}O_9P_3Ru_3$
M_r	967.71	1057.9	1057.9	1220.1	1371.9	1099.9
Crystal system	Monoclinic	Orthorhombic	Triclinic	Monoclinic	Orthorhombic	Monoclinic
Space group	$P2_1/n$ (No. 14)	*Pbca* (No. 61)	$P\bar{1}$ (No. 2)	$P2_1/c$ (No. 14)	*Pbca* (No. 61)	$P2_1/n$ (No. 14)
a (Å)	13.064(2)	20.970(4)	20.28(1)	18.679(4)	20.930(7)	12.7920(9)
b (Å)	11.765(1)	26.370(7)	17.33(2)	16.005(4)	33.890(5)	24.510(2)
c (Å)	23.601(3)	15.317(5)	12.65(1)	18.816(4)	15.524(3)	14.152(2)
α (°)			93.5(1)			
β (°)	103.830(3)		98.93(5)	114.71(2)		94.328(8)
γ (°)			102.94(9)			
V (Å^3)	3522	8470	4258	5110	11 011	4430
D_c (g cm^{-3})	1.825	1.659	1.650	1.586	1.655	1.649
Z	4	8	4	4	8	4
μ_{Mo} (cm^{-1})	14.2	12.2	12.1	10.2	11.5	11.7
Specimen (mm)	0.35 × 0.24 × 0.14	0.30 × 0.24 × 0.18	0.04 × 0.75 × 0.25	0.32 × 0.37 × 0.35	0.40 × 0.30 × 0.45	0.58 × 0.38 × 0.27
$T_{min,\ max}$	0.65, 0.86	0.77, 0.83	0.76, 0.95	0.70, 0.77	0.62, 0.72	0.66, 0.84
$2\theta_{max}$ (°)	75	60	50	65	55	75
$N_{(unique)}$ [a]	18 414	12 318	14 932	18 500	12 598	23 196
$N(I > 3\sigma(I))$	15 446	6773	6266	11 067	6902	20 151
R	0.034	0.045	0.098	0.054	0.048	0.044
R_w	0.066	0.046	0.10	0.059	0.056	0.108

[a] N_{tot}, R = 71 704, 0.030, **1**; 88 126, 0.044, **2d**.

recorded without further discussion. The second, more precise, determination was carried out on a more substantial orthorhombic (*Pbca*) prism and has one complete molecule in the asymmetric unit. Complexes **2b** and **2c** crystallised in space groups monoclinic $P2_1/c$ and orthorhombic *Pbca* (as the bis-dichloromethane solvate), respectively, also having one complete molecule in each asymmetric unit. Their geometries are given in Table 2 in comparison with those of **1**, redetermined here at low temperature, and [$Ru_3(\mu\text{-dppm})(CO)_9(PPh_2(C_6H_4R'\text{-}2)$] [3] (**2e**, R′ = CHO; **2f**, R′ = NHC(O)Ph). All the complexes, **2**, have dppm ligands occupying equatorial sites with the introduced phosphine ligand, at the previously unsubstituted Ru atom, also equatorial, but significantly out of plane, on the opposite side to C(0).

The triangular ruthenium arrays found for complexes **2** contain two shorter and one longer Ru–Ru interaction. The latter, Ru(2)–Ru(3), in each case lying directly adjacent to the introduced phosphine seemingly correlated to the phosphine steric encumbrance with the largest ligands, viz PCy_3, $PPh_2(C_6H_4R'\text{-}2)$ and PPr^i_3, inducing the greatest lengthening relative to the parent compound **1**. The effect is also exhibited by the complexes containing the smaller ligands, in spite of their substantially smaller cone angles (PEt_3 132°, PPh_3 145°). The shorter bonds [2.827(2)–2.8592(9) Å] appear relatively unaffected by the nature of the introduced ligand compared with the Ru–Ru separations in other tri-substituted phosphine clusters [13,14] where the metal–metal bonds, although longer than in the parent carbonyl [$Ru_3(CO)_{12}$], show no apparent correlation with phosphine ligand cone angle.

The variation in Ru(n)–P(n) dppm (n = 1, 2) distances is trivial, falling between 2.311(2) and 2.336(2) Å. By contrast the nature of the introduced phosphine has a pronounced effect on the Ru(3)–P(3) bond length which increases with the size of the phosphine ligand. The smallest ligand (PEt_3) is also more basic than the aryl phosphines and as such might be expected to donate more electron density, concomitantly enhancing the effects of back donation, and shortening the Ru–P bond. However, it seems that the extreme cone angle of PCy_3 (170°) dominates electronic considerations, resulting in the longest distance of 2.397(2) Å. The electronic effects of the introduced ligands might also be better evident in the Ru–CO distances because of the π-acidity of the carbonyl ligand. The length of M–CO_{eq} bonds *cis* to a Group 15 ligand [15] and in an equatorial site, can act as a reliable indicator of the relative degree of backbonding. In the parent **1**, distances on the unsubstituted Ru atom are significantly longer than Ru(3)–$C(31)_{eq}$ in complexes **2a**, **b**, **d** which contain the alkyl phosphines, but no such effect is seen for the PPh_3 adduct (**2c**).

3.3. Cluster activation

The bidentate nature of the dppm ligand effectively tethers the Ru(1)–Ru(2) bond for all clusters **2**, unlike other unidentate trisubstituted clusters which have more flexibility in their metal framework and can diminish

Table 2
Bond lengths (Å), angles (°) and torsion angles (°) for complexes **1** and **2** [a]

L	CO (**1**)	PEt$_3$ (**2a**) [b]	PCy$_3$ (**2b**)	PPh$_3$ (**2c**)	PPr^i (**2d**)	PPh$_2$ (C$_6$H$_4$R$_1$)^2 (**2e**)	PPh$_2$ (C$_6$H$_4$R$_2$)^2 (**2f**)
Bond lengths							
Ru(l)–Ru(2)	2.8377(3)	2.8523(8)	2.8476(8)	2.835(1)	2.8756(3)	2.8343(9)	2.8421(9)
Ru(l)–Ru(3)	2.8406(4)	2.8540(8)	2.8587(8)	2.8592(9)	2.8586(5)	2.8541(9)	2.827(2)
Ru(2)–Ru(3)	2.8640(4)	2.8733(8)	2.9060(9)	2.8697(9)	2.9076(4)	2.899(1)	2.9272(9)
Ru(1)–P(l)	2.3191(6)	2.330(1)	2.325(2)	2.331(2)	2.3170(8)	2.316(2)	2.316(2)
Ru(2)–P(2)	2.3288(7)	2.313(1)	2.333(1)	2.311(2)	2.3235(8)	2.327(2)	2.336(2)
Ru(3)–P(3)	1.929(3) [c]	2.348(2)	2.397(2)	2.360(2)	2.3852(8)	2.359(2)	2.340(2)
Ru(1)–C(11)$_{eq}$	1.913(2)	1.879(7)	1.874(7)	1.893(7)	1.875(5)	1.875(6)	1.864(7)
Ru(1)–C(12)$_{ax}$	1.924(2)	1.899(6)	1.926(6)	1.918(8)	1.918(4)	1.935(6)	1.897(7)
Ru(1)–C(13)$_{ax}$	1.945(3)	1.928(6)	1.921(6)	1.927(7)	1.933(3)	1.921(6)	1.913(7)
Ru(2)–C(21)$_{eq}$	1.917(3)	1.881(5)	1.877(6)	1.882(8)	1.896(4)	1.889(6)	1.869(6)
Ru(2)–C(22)$_{ax}$	1.929(2)	1.907(5)	1.938(7)	1.921(8)	1.937(4)	1.908(7)	1.915(7)
Ru(2)–C(23)$_{ax}$	1.928(2)	1.921(7)	1.904(6)	1.927(8)	1.928(3)	1.903(7)	1.911(7)
Ru(3)–C(31)$_{eq}$	1.915(3)	1.858(7)	1.865(6)	1.889(9)	1.869(3)	1.861(6)	1.870(6)
Ru(3)–C(32)$_{ax}$	1.945(3)	1.889(6)	1.929(7)	1.911(8)	1.923(3)	1.904(6)	1.924(7)
Ru(3)–C(33)$_{ax}$	1.947(3)	1.916(7)	1.934(7)	1.924(8)	1.932(3)	1.913(7)	1.905(7)
C–O$_{ax}$ (av.)	1.13	1.14	1.13	1.13	1.15	1.14	1.15
C–O$_{eq}$ (av.)	1.14	1.14	1.13	1.14	1.14	1.15	1.15
Bond angles							
Ru(1)–Ru(2)–Ru(3)	59.760(9)	59.79(2)	59.57(2)	60.16(2)	59.243(8)	59.70(2)	58.66(3)
Ru(2)–Ru(l)–Ru(3)	60.580(6)	60.47(2)	61.23(2)	60.53(2)	60.936(7)	61.27(3)	62.17(3)
Ru(2)–Ru(3)–Ru(1)	59.66(1)	59.74(2)	59.20(2)	59.32(3)	59.821(9)	59.03(2)	59.16(2)
Ru(1)–Ru(2)–P(2)	89.17(1)	91.06(4)	87.60(4)	90.93(5)	94.18(2)	87.84(5)	86.76(5)
Ru(2)–Ru(1)–P(1)	95.55(1)	95.39(4)	95.36(4)	94.97(5)	92.22(2)	96.17(5)	95.97(5)
Ru(2)–Ru(3)–P(3)	104.18(9) [c]	103.85(5)	111.81(4)	105.35(6)	114.49(2)	108.61(4)	117.28(5)
P(1)–Ru(1)–C(11)	100.53(7)	105.0(2)	104.3(2)	106.9(2)	104.5(2)	101.6(4)	100.1(3)
P(1)–Ru(1)–C(12)	91.68(6)	92.3(2)	94.8(2)	92.5(2)	91.3(1)	91.3(2)	93.5(3)
P(1)–Ru(1)–C(13)	92.41(7)	90.6(2)	89.7(2)	89.8(2)	91.9(1)	92.5(2)	91.9(3)
P(2)–Ru(2)–C(21)	103.47(9)	100.3(2}	98.8(2}	101.1(2)	99.4(1)	98.2(2)	97.8(3)
P(2)–Ru(2)–C(22)	97.20(3)	95.3(2)	100.8(2)	95.1(3)	91.3(1)	99.1(2)	98.3(2)
P(2)–Ru(2)–C(23)	88.47(7)	91.4(2)	91.3(2)	90.1(2)	93.9(1)	91.4(2)	90.7(3)
P(3)–Ru(3)–C(31)	104.8(1) [c]	102.0(2)	102.1(2)	102.2(3)	100.7(1)	101.0(2)	101.3(3)
P(3)–Ru(3)–C(22)	90.5(1) [c]	91.0(2)	89.5(2)	94.7(3)	88.10(9)	93.5(2)	86.1(2)
P(3)–Ru(3)–C(33)	92.7(1) [c]	89.1(2)	89.7(2)	87.3(2)	88.56(9)	89.8(2)	93.0(2)
Ru(3)–Ru(1)–C(11)	104.07(7)	99.5(2)	100.6(2)	99.2(2)	102.6(2)	101.4(2)	102.3(3)
Ru(3)–Ru(1)–C(12)	89.75(6)	92.3(2)	91.2(2}	98.2(2)	88.6(1)	96.9(2)	90.8(2)
Ru(3)–Ru(1)–C(13)	84.35(6)	84.2(2)	82.5(2)	79.7(2)	87.9(6)	77.9(2)	82.1(3)
Ru(3)–Ru(2)–C(21)	108.88(8)	108.8(2)	114.4(2)	107.8(2)	107.5(1)	114.7(2)	118.0(3)
Ru(3)–Ru(2)–C(22)	77.07(7)	81.8(2)	80.0(2)	85.4(2)	86.8(1)	78.9(2)	72.2(2)
Ru(3)–Ru(2)–C(23)	97.11(7)	90.2(2)	88.6(2)	88.1(2)	86.8(1)	91.1(2)	99.0(2)
Torsion angles							
P(3)–Ru(3)–Ru(1)–P(1)	50.3(3) [c]	33.3(2}	62.5(2)	43.9(3)	13.4(2)	−70.41(1)	−96.15(4)
P(3)–Ru(3)–Ru(2)–P(2)	−146.9(1) [c]	−167.8(1)	−163.4(1)	−176.6(1)	−168.77(5)	156.8(1)	141.2(1)
P(1)–Ru(1)–Ru(2)–P(2)	19.34(2)	9.8(1)	17.4(1)	14.0(1)	8.59(3)	−19.2(1)	−22.9(1)
P(3)–Ru(3)–Ru(2)–C(21)	19.7(1) [c]	5.8(2)	16.7(2)	1.1(3)	7.6(1)	−17.0(3)	−20.1(3)
C(31)–Ru(3)–Ru(2)–C(21)	−140.5(2)	−164.0(5)	−156.1(5)	−174.2(6)	−169.3(2)	−13.5(2)	−29.0(3)
C(0)–P(l)–Ru(1)–Ru(2)	−0.3(1)	8.4(2)	6.3(2)	3.7(2)	−23.6(1)	0.15(1)	4.60(1)
C(0)–P(2)–Ru(2)–Ru(1)	−37.27(8)	−27.5(2)	−40.5(2)	−31.3(2)	6.9(1)	37.81(1)	40.38(1)

[a] $R_1 = CHO$; $R_2 = NHCOPh$.
[b] Orthorhombic form.
[c] For P(3) read C(34).

steric strain by twisting their ML$_4$ units, moving from D_{3h} to D_3 symmetry. This is also the case in the parent carbonyl, [Ru$_3$(CO)$_{12}$], which can accommodate the steric constraints of its Ru(CO)$_4$ groups by twisting of the core to disentangle the equatorial carbonyls. However, in **1**, it seems that there is substantial steric interaction of the equatorial CO with the bulky dppm ligand, which may activate the equatorial CO group to further phosphine substitution, the longer Ru–P distance alleviating the crowding. The degree of flexibility present within the dppm ligand may assist in the release of steric encumbrance about Ru(3) on passing from CO on Ru(3) to the larger cone angle ligands; the P(1)–Ru(1)–Ru(2)–P(2) torsion angles appear to increase as a function of phosphine cone angle.

The mechanism by which CO substitution occurs has been examined in an exhaustive and quantitative manner by Pöe and co-workers [12,14,16]. In a series of papers they have determined that the CO substitution mechanism of $[Ru_3(CO)_{10}(L)_2]$ to give $[Ru_3(CO)_{10}L'(L)_2]$ (L, L′ = tertiary phosphine) is a dissociative one involving a $(Ru_3(CO)_9(L)_2)\cdots CO$ transition state. They were able to separate steric and electronic effects and suggest that the steric repulsions in the transition state are only marginally less than in the ground state.

4. Conclusion

Enhanced reactivity of $[Ru_3(\mu\text{-dppm})(CO)_{10}]$ over the parent carbonyl $[Ru_3(CO)_{12}]$ appears to be a result of its inability to effectively relieve steric congestion imposed by the presence of the bulky, bidentate dppm ligand. This hinders the mutual twisting of $Ru(CO)_3(P)$ units and is manifested by a lengthening of Ru(3)–Ru(2). Thus the equatorial CO group is more susceptible to substitution than those in $[Ru_3(CO)_{12}]$. Presumably this has the effect of activating Ru(3)–Ru(2) to further reaction by cannibalisation of the dppm ligand in the absence of a suitable donor.

5. Supplementary material

Crystallographic data for the structural analyses have been deposited with the Cambridge Crystallographic Data Centre, CCDC Nos. 177736–41. Copies of this information may be obtained free of charge from The Director, CCDC, 12 Union Road, Cambridge CB2 1EZ, UK (fax: +44-1223-336033; e-mail: deposit@ccdc.cam.ac.uk; or www: http://www.ccdc.cam.ac.uk).

Acknowledgements

We thank the Department of Chemistry for a start up grant (GAK). ASH is the holder of a Australian Postgraduate Award and a University Postgraduate Supplementary Award. AAT thanks Zanjan University for a study leave grant.

References

[1] A.W. Coleman, D.F. Jones, P.H. Dixneuf, C. Brisson, J.-J. Bonnet, G. Lavigne, Inorg. Chem. 23 (1984) 952.
[2] M.I. Bruce, J.R. Hinchliffe, B.W. Skelton, A.H. White, J. Organomet. Chem. 495 (1995) 141.
[3] C.J. Adams, M.I. Bruce, P.A. Duckworth, P.A. Humphrey, O. Kuhl, E.R.T. Tiekink, W.R. Cullen, P. Braunstein, S.C. Cea, B.W. Skelton, A.H. White, J. Organomet. Chem. 467 (1994) 251.
[4] M.I. Bruce, P.A. Humphrey, R.J. Surynt, E.R.T. Tiekink, Aust. J. Chem. 47 (1994) 477.
[5] O. bin Shawkataly, S.G. Teoh, H.K. Fun, J. Organomet. Chem. 464 (1994) C25.
[6] M.I. Bruce, P.A. Humphrey, B.W. Skelton, A.H. White, M.L. Williams, Aust. J. Chem. 38 (1985) 1301.
[7] N. Lugan, J.-J Bonnet, J.A. Ibers, J. Am. Chem. Soc. 107 (1985) 4484.
[8] N. Lugan, J.-J. Bonnet, J.A. Ibers, Organometallics 7 (1988) 1538.
[9] M.I. Bruce, B.K. Nicholson, M.L. Williams, Inorg. Synth. 26 (1990) 225.
[10] S.R. Hall, G.S.D. King, J.M. Stewart, XTAL3.4 User Manual, Lamb, University of Western Australia, Australia Perth, 1995.
[11] D.F. Foster, J. Harrison, B.S. Nicholls, A.K. Smith, J. Organomet. Chem. 295 (1985) 99.
[12] B. Ambwani, S.K. Chawla, A.J. Pöe, Inorg. Chim. Acta 133 (1987) 93.
[13] M.I. Bruce, M.J. Liddell, O.B. Shawkataly, C.A. Hughes, B.W. Skelton, A.H. White, J. Organomet. Chem. 347 (1988) 207.
[14] N.M.J. Brodie, A.J. Pöe, Can. J. Chem. 73 (1995) 1187.
[15] M.I. Bruce, M.J. Liddell, C.A. Hughes, B.W. Skelton, A.H. White, J. Organomet. Chem. 347 (1988) 157.
[16] B. Ambwani, S.K. Chawla, A.J. Pöe, Polyhedron 7 (1988) 1939.